

## PHYSICS OF FLUID SPREADING ON ROUGH SURFACES

K. M. HAY AND M. I. DRAGILA

**Abstract.** In the vadose zone, fluids, which can transport contaminants, move within unsaturated rock fractures. Surface roughness has not been adequately accounted for in modeling movement of fluid in these complex systems. Many applications would benefit from an understanding of the physical mechanism behind fluid movement on rough surfaces. Presented are the results of a theoretical investigation of the effect of surface roughness on fluid spreading. The model presented classifies the regimes of spreading that occur when fluid encounters a rough surface: i) microscopic precursor film, ii) mesoscopic invasion of roughness and iii) macroscopic reaction to external forces. Theoretical diffusion-type laws based on capillarity and fluid and surface frictional resistive forces developed using different roughness shape approximations are compared to available fluid rise on roughness experiments. The theoretical diffusion-type laws are found to be the same apparent functional dependence on time; methods that account for roughness shape better explain the data as they account for more surface friction.

**Key Words.** roughness, wetting, capillarity

### 1. Introduction

The movement of fluids in unsaturated rock fractures is an involved subject, requiring an understanding of multiphase fluid dynamics and fluid interaction with soil and porous media as well as the use of complex modeling systems. However, before one can model the big picture of multiphase flow in a rock fracture system it is important to understand the basic physics that describes types of fluid movement and interaction with boundaries. In a fractured rock system, the rock surface can be porous, moist, chemically heterogeneous and rough. In this manuscript the focus will be the movement of a wetting fluid over a rough surface. Glass is commonly used to model rock when investigating characteristics of droplet movement in rock fractures. It has been observed that the speed of droplets moving down between smooth glass parallel plates is significantly different than the speed down rough glass plates and rock fractures. The physical mechanism behind fluid movement on rough surfaces is not yet well understood.

A wetting fluid is pulled into roughness by capillarity. What are the physical mechanisms that drive and resist this movement? An analytical diffusion-type law is developed that provides an explanation and a way to quantify the physical mechanisms that drive fluid invasion into roughness. The theory is based on the balance between capillary and fluid and surface frictional resistive forces. Relationships derived have the same apparent functional dependence on time as available experiments of fluid rise on roughness. The more accurate the geometry of the roughness shape, the better explain the data.

There is a large body of experimental and theoretical literature that clearly shows a rough surface affects fluid movement. Wenzel [1] observed that surface roughness caused a hydrophobic fluid to behave as if it were more hydrophobic and a hydrophilic fluid to behave as if it were more hydrophilic. Wenzel also suggested that the structure of the surface had a greater effect on the static contact angle than the chemistry. Bico *et al.* [2] suggest that a surface can be designed to tune its wetting properties. They observe the dynamic behavior of the gas-liquid-solid interface for a hydrophilic fluid on a rough surface and derive a spreading diffusion law based on the change in energy that accompanies movement of the contact line. Cazabat and Cohen Stuart [3] explored the effects of surface roughness experimentally. They found that drops on rough surfaces spread faster than drops on smooth surfaces. While the macroscopic cap of the drop on a rough surface follows a gravity-dominated behavior, a thin fluid front rushes away from the macroscopic edge, spreading *into* the roughness by capillarity. Eventually fluid in the macroscopic drop relaxes onto the fluid film that invaded the roughness.

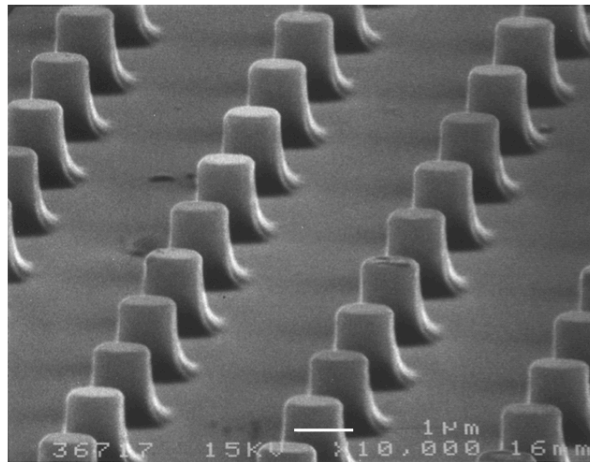


FIGURE 1. Microstructure with regular micronic cylindrical spikes used for the experiment [2].

The model for the invasion process incorporates the capillary driving mechanism suggested by experimentalists and theoreticians in this field [2], [3]. The expression derived uses an idealized geometry for the rough surface that coincides with the micropatterned surface used in experiments by Bico *et al.* [2] (Figure 1). The goal of the mathematical model is to predict the wetting behavior on a surface, given the basic surface structure and to eventually describe larger multiphase systems involving rock surfaces [4].

## 2. Theory

The model presented classifies three regimes of spreading: precursor film, roughness invasion and reaction to external forces (Fig. 2). It is known that a microscopic *precursor film* precedes a fluid that is in contact with a solid. Movement of the precursor film is governed by molecular diffusive transport of vacancies from the tip of the film to the edge of the macroscopic meniscus [5]. It is assumed here that the precursor film must also occur on rough surfaces and this will be considered the first regime of spreading. During the second regime of spreading on a rough

surface, the gravity-independent *mesoscopic fluid invasion*, the fluid moves into the rough texture and this regime is the focus of this study. The third regime begins when the macroscopic meniscus relaxes into its new shape or location governed by external forces, such as gravity.

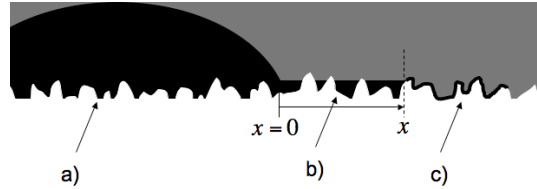


FIGURE 2. Spreading fluid drop (black) on a rough surface (white), not to scale. a) macroscopic passive drop; b) Mesoscopic fluid invasion regime (fills in the roughness); c) Precursor film (on the order of 100 Angstroms thick).

The rough surface shown in Figure 1 is idealized here as comprised of a series of small cylindrical posts lined up on an otherwise smooth surface. The fluid movement through the idealized rough surface is further simplified theoretically by modeling the surface as a series of parallel channels. This approach has been used historically in porous media by Washburn [6]. The model assumes that invasion into the rough surface is driven solely by capillary forces; gravity is ignored for this regime. Other simplifying assumptions made: the system is isothermal, solid, liquid and vapor elements are chemically homogeneous and there is no evaporation.

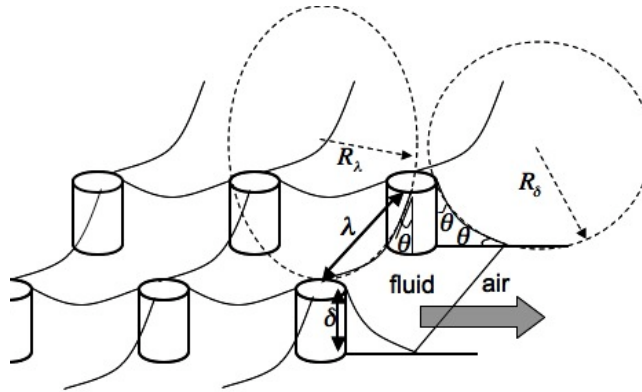


FIGURE 3. Illustration of the fluid-air interface created by the presence of roughness. All gas-fluid-solid contact angles ( $\theta$ ) are identical. Interface curvature creates capillarity and drives flow. Fluid movement is in the direction of the shaded arrow. Determination of the radius of curvature is governed by  $\lambda$  and  $\delta$ .

**2.1. Capillary driving mechanism.** A constant capillary force exerted at the wetting front is assumed to pull fluid into roughness (invasion). The capillary force is calculated using the curvature of the fluid-gas interface. The radius of curvature is

completely described by the height of the cylinders ( $\delta$ ) and the separation between cylinders ( $\lambda$ ) and the static gas-liquid-solid contact angle ( $\theta$ ). This force per unit area is defined by the Young-Laplace equation,

$$(1) \quad \Delta P_c = \gamma \left( \frac{1}{R_\delta} + \frac{1}{R_\lambda} \right),$$

where  $\Delta P_c$  is the pressure difference across the fluid-air interface caused by capillarity,  $\gamma$  is the liquid-gas surface tension, and  $R_\delta$  and  $R_\lambda$  are the radii of curvature. If the cylinders are normal to the smooth surface (see Figure 3) and assuming the pressure in the bulk macroscopic fluid equals the external (atmospheric) pressure then the force per unit area driving the fluid into the rough texture is [4]

$$(2) \quad \Delta P_c = \gamma \left( \frac{(2\delta + \lambda) \cos \theta - \lambda \sin \theta}{\delta \lambda} \right).$$

**2.2. Various friction approximations.** In this section, the viscous dissipation generated from fluid flow is calculated. The strength of viscous dissipation is a function of the geometry of the surface. In modeling, it is of interest to use the simplest geometry that captures the behavior. For this purpose we compare results of four geometries (of varying complexity) to the experimental results. One geometry is that of a flat surface with no roughness elements, the remainder use channel approximations.

First, a hydraulic diameter formulation is used to approximate the complex geometry of the surface (the no-slip boundary) that is in contact with the moving fluid. The hydraulic diameter method approximates a non-circular flow duct (in this case a rectangular channel) as a cylinder with an effective radius that requires knowledge of the geometry of the system, comparing the wetted area to the wetted perimeter to give a reasonable estimate of friction.

Application of the Navier-Stokes Equation for an arbitrarily shaped channel leads to a relationship between a constant pressure gradient,  $\Delta P$ , across the invading fluid and the velocity of the invading fluid front,  $U$ , in the form

$$(3) \quad \Delta P_\mu = \frac{2P_0\mu U \Delta x}{d_h^2},$$

where  $x$  is the distance from the macroscopic edge of the bulk fluid to the invasion front (see Figure 2),  $\mu$  is the dynamic viscosity,  $d_h$  is the hydraulic diameter and  $P_0$  is the Poiseuille number [7]. Both  $d_h$  and  $P_0$  are specified by the surface geometry. The pressure gradient results from the decrease in pressure in the fluid at the fluid-air interface caused by capillarity, described by Equation 2. Solving for the velocity,  $U$ , of the front edge of the invading fluid yields

$$(4) \quad U = \frac{\gamma d_h^2}{2P_0\mu x} \left( \frac{(2\delta + \lambda) \cos \theta - \lambda \sin \theta}{\delta \lambda} \right).$$

Note that in the case of vertical imbibition, the lower boundary for the roughness driven invasion is  $x_0 = \kappa^{-1}$ , where  $\kappa^{-1}$  is the capillary length given by  $(\gamma/\rho g)^{1/2}$ . Even on a flat surface the wetting front will move up by a height of  $\kappa^{-1}$ . Integrating Equation 4 leads to a diffusion-type film invasion rate,

$$(5) \quad x_h = \left[ \frac{\gamma d_h^2}{P_0\mu} \left( \frac{(2\delta + \lambda) \cos \theta - \lambda \sin \theta}{\delta \lambda} \right) \right]^{1/2} t^{1/2} + x_0.$$

where  $t$  is the time it takes for the edge of the fluid to travel the distance  $x$  along the textured surface away from the macroscopic edge of the bulk fluid and the subscript  $h$  denotes the use of hydraulic diameter method to approximate the frictional resistance [4].  $x \propto t^{1/2}$  is the solution to a diffusion equation. Diffusion is

a process which describes any movement driven by an energy gradient where the energy difference is constant but the distance over which the gradient is expressed grows. Diffusion is often used to describe the process of heat transport in a fluid or mass transport in the mixing of fluids due to molecular brownian motion [7]. In this fluid invasion of roughness case, mass is transported away from the bulk fluid driven by a pressure gradient imposed by capillarity. Physically, this solution form means that the fluid movement slows as the invasion front gets further and further from the bulk fluid.

The Poiseuille number and the hydraulic diameter must be known to calculate the diffusion coefficient (the entire term in front of  $t^{1/2}$  in Equation 5). The Poiseuille number,  $P_0$ , is 14.38 for a rectangle with an aspect ratio of  $\alpha = \delta/\lambda = 0.48$  [8] as is the case for the experiment used here. The hydraulic diameter is [4]

$$(6) \quad d_h = \frac{4A}{P_w} = \frac{4 \left[ \lambda \delta - \frac{\lambda^2}{4} \left( \frac{\frac{\pi}{2} - \theta}{\cos \theta} - \tan \theta \right) \right]}{2\delta + \lambda},$$

where the cross-sectional area of the flow,  $A$ , was approximated as a rectangle with vertical walls of height  $\delta$  and width  $\lambda$  minus the area of a circular segment determined by the contact angle (Figure 4 e) and the wetting perimeter,  $P_w = 2\delta + \lambda$ . For a simple rectangle,  $d_h = 4\delta\lambda/(2\delta + \lambda)$  (Figure 4 d).

If the elements are rounded, the same equation (6) can be used by substituting  $\theta$  for  $\theta + \theta'$  where  $\theta'$  is the angle of inclination of the cylinder top (Figure 4 f) [4].

Another modeling option is to approximate the roughness as a semi circular channel. The no-slip boundary is applied along the entire semi-circular perimeter. Specifically, a *Hagen-Poiseuille half pipe flow* model gives the following function for the spreading distance,

$$(7) \quad x_{H-P} = \left[ \frac{\gamma \delta^2}{4\mu} \left( \frac{(2\delta + \lambda) \cos \theta - \lambda \sin \theta}{\delta \lambda} \right) \right]^{1/2} t^{1/2} + x_0.$$

where the radius of the pipe has been approximated as the height of the obstacles,  $\delta$  (see Figure 4 c), the subscript  $H - P$  denotes the use of the Hagen-Poiseuille pipe flow approximation for the frictional resistance term. This approximation may be more adequate in naturally textured surfaces (e.g. rock) than for a surface such as shown in Figure 1, because natural systems are likely to have less severe vertical edges. A downfall of this method is that a pipe flow approximation will become less accurate for systems with obstruction heights not comparable to the half-width separation between obstructions. The experiment used for comparison to these theories has  $\delta = 1.2\mu m$  and half-width distance,  $\lambda/2 = 0.125\mu m$ .

The simplest geometry is that of a *Poiseuille film flow* (Figure 4 b). The equation for the spreading distance becomes

$$(8) \quad x_P = \left[ \frac{2\delta^2 \gamma}{3\mu} \left( \frac{(2\delta + \lambda) \cos \theta - \lambda \sin \theta}{\delta \lambda} \right) \right]^{1/2} t^{1/2} + x_0,$$

where the subscript  $P$  denotes the use of the Poiseuille film flow approximation [4]. Approximating the flow in the roughness as a film ignores dissipation caused by the presence of the cylinders and only accounts for no-slip condition along a smooth plate (see Figure 4 b) and is thus expected to overestimate the rate of invasion.

### 3. Comparison to experiment

Experiments to test this concept consist of a rough microstructured surface (Figure 1) that was brought into contact with a reservoir of silicon oil. The upward

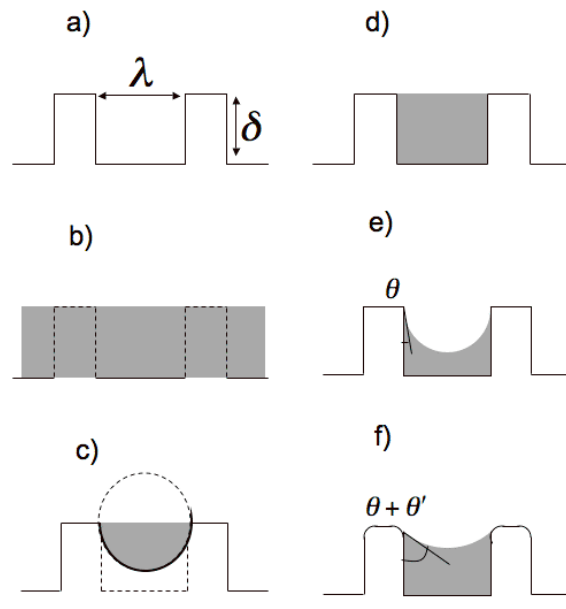


FIGURE 4. Various cross-sectional channel flow models used to estimate viscous dissipation. The solid line represents the shape of the ideal rough surface (height  $\delta$ , width  $\lambda$ ), the shaded region is the fluid. a) The rough surface, no fluid; b) Poiseuille film flow; c) Hagen-Poiseuille half-pipe flow; d) Hydraulic diameter approximation, rectangle; e) Hydraulic diameter, static contact angle off the vertical wall; f) Hydraulic diameter, static contact angle plus  $\theta'$ .

rate of fluid invasion into the rough surface is not dependent on surface orientation [3], [2]. Figure 5 compares the experimental data of Bico *et al* (2001) with each of the theoretical spreading equations.

Values for the diffusion coefficients for Equations 5, 7 and 8 can be calculated using parameters from the experimental set up of Bico *et al* [2]: surface tension,  $\gamma = 20.6 \times 10^{-3} N/m$ ; density,  $\rho = 950 kg/m^3$ ; advancing contact angle,  $\theta = 0$ ; dynamic viscosity,  $\mu = 16 \times 10^{-3} Pa \cdot s$ ; height of the cylinders,  $\delta = 1.2 \times 10^{-6} m$ ; radius of cylinders,  $R = 0.5 \times 10^{-6} m$ ; and distance between cylinder edges,  $\lambda = 2.5 \times 10^{-6} m$  (separation between cylinder centers =  $\lambda + 2R$ ).

Values for each theoretical diffusion coefficient correspond to the slope of the curves in Figure 5 and are listed on the figure. The data fits well to a curve that has the same functional dependence as the theories and a slope of  $2.7 \times 10^{-4} m \cdot s^{-1/2}$ .

**3.1. Discussion.** Regardless of the method used for approximating the resisting fluid friction, all the theoretical spreading equations result in diffusion laws of the form  $x \propto t^{1/2}$ , having the same apparent functional time dependence as the experimental data of Bico *et al*.

The half-pipe flow model is slower than the film flow model because pipe geometry provides for greater contact area although it still doesn't account for the

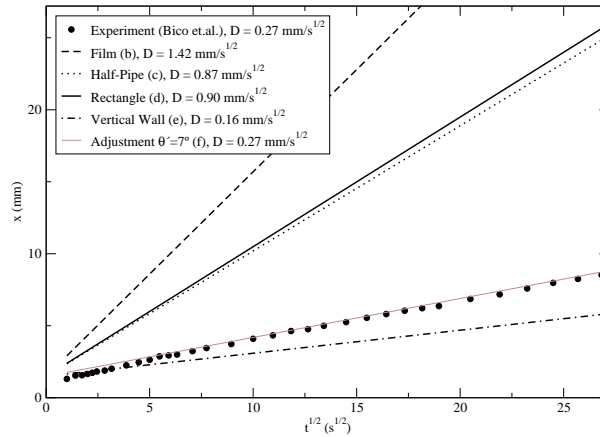


FIGURE 5. Data acquired by Bico *et al* [2]. Data is compared to various theoretical diffusion-type models,  $x = Dt^{1/2} + x_0$ , where  $D$ , the diffusion coefficient, equals the slope of the line. Corresponding geometry illustrations from Fig. 4 are included in the legend. The theories here have  $x_0 = 1.5\text{mm}$ , corresponding to the theoretical capillary length.

rectangular shape of the cylinder edges. An effective hydraulic diameter approximation provides a more realistic boundary condition than film or pipe flow and also allows for freedom in describing the approximated channel shape and fluid shape.

The hydraulic diameter approximation that uses the contact angle off the vertical wall to govern the shape predicts a diffusion coefficient that is smaller than the data. Allowing a corner angle adjustment of  $\theta' = 7^\circ$ , increases the wetting area compared to wetting perimeter, and gives a close fit to the data. However, a precise match created by an arbitrary adjustment to the cylinder geometry may be fortuitous because the discrepancy between the theories and the data may be an indication of unaccounted for physical mechanisms. There remain several unaccounted for features such as an uneven advancing fluid front, small scale fluid dynamics, vertical fluid motion, and allotment for non-channelized approximation which are further discussed in Hay *et al.* [4].

#### 4. Summary

It is the intention of this research to eventually explain the movement of the air-water interface occupying the space between rock fractures. This has applications to fluid transport through rock fractures, then on a larger scale, transport of fluid from the ground surface to groundwater, estimating the transport characteristics of contaminants. To this end, the first issue that needs to be addressed is the physical mechanism behind fluid flowing over a rough surface.

This investigation compares predictions by a theoretical model for a fluid invasion on a rough surface to experiments. The rate of spreading on a rough surface can be predicted given the surface tension, viscosity, contact angle and geometry of the surface. It is the nature of roughness in natural systems to be random and possibly fractal-like. This provides serious challenges in attempting to theoretically quantify

the wetting behavior over these surfaces. Idealizing the structure is one step closer to understanding this complex fluid movement. Results indicate that a hydraulic diameter approach, because of its flexibility in representing complex shapes may be very useful as long as the shape of the free surface is properly accounted for. Fluid movement suggested here describes the fluid invasion process that occurs when a wetting fluid encounters roughness but may not affect the overall speed of a fluid droplet between parallel plates, except by possibly changing the contact angle. This issue is being investigated further.

We thank Dr. José Bico for the use of his experimental data, Zachary Wiren for the many conceptual discussions that lead to improving the invasion theory and the NSF (Grant 0449928) for financial support.

### References

- [1] R. N. Wenzel, Resistance of Solid Surfaces to Wetting by Water, *Ind. Eng. Chem.*, 28 (1936) 988-994.
- [2] J. Bico, C. Tordeux, and D. Quéré, Rough Wetting, *Europhys. Lett.*, 55 (2001) 214-220.
- [3] A. M. Cazabat, and M.-A. Cohen Stuart, Dynamics of Wetting: Effects of Surface Roughness, *Journal of Phys. Chem.*, 90 (1986) 5845-5849.
- [4] K. M. Hay, M. I. Dragila, J. Liburdy, A Theoretical Model for the Wetting of a Rough Surface, To appear in *Journal of Colloid and Interface Science*.
- [5] S. F. Burlatsky, G. Oshanin, A.-M. Cazabat, and M. Moreau, Microscopic Model of Upward Creep of an Ultrathin Wetting Film, *Phys. Rev. Lett.*, 76 (1996) 86-89.
- [6] E. W. Washburn, The Dynamics of Capillary Flow, *Phys. Rev.* 17 (1921) 273-283.
- [7] F. M. White, *Viscous Fluid Flows*, McGraw-Hill, Boston, 1991.
- [8] R. K. Shah, A. L. London, *Advances in Heat Transfer*, Academic Press, New York, NY, 1978.

Department of Physics, Oregon State University, Corvallis, Oregon

Department of Crop and Soil Sciences, Oregon State University, Corvallis, Oregon